

LASER PHASE ERRORS IN SEEDED FELS

D. Ratner, A. Fry, G. Stupakov, W. White, SLAC, Menlo Park, California 94025, USA

Abstract

Harmonic seeding of free electron lasers has attracted significant attention as a method for producing transform-limited pulses in the soft X-ray region. Harmonic multiplication schemes extend seeding to shorter wavelengths, but also amplify the phase errors of the initial seed laser, and may degrade the pulse quality and impede production of transform-limited pulses. In this paper we consider the effect of seed laser phase errors in high gain harmonic generation and echo-enabled harmonic generation. We use simulations to confirm analytical results for the case of linearly chirped seed lasers, and extend the results for arbitrary seed laser envelope and phase.

INTRODUCTION

The recent success of Self-Amplified Spontaneous Emission (SASE) Free Electron Lasers (FELs) has led to x-ray sources of unprecedented brightness [1, 2]. However, some applications still require higher power (e.g. [3, 4]), and the poor longitudinal coherence of SASE FELs can inhibit x-ray optimization and degrade experimental results. To improve control over the spectral and temporal x-ray properties, there is strong interest in seeding FELs at high harmonics of optical or UV lasers. Beamline users are particularly interested in the minimal bandwidth and simple temporal structure of transform-limited x-ray pulses.

One potentially serious issue for the seeding process is how properties of the seed laser can affect the production of transform-limited x-ray pulses. In Ref. [5] we presented a detailed study of how laser phase errors affect the final pulse characteristics. Here we present a summary of those results.

There are numerous challenges for seeding schemes, and previous theoretical and experimental studies have focused on a wide variety of accelerator and FEL requirements. In particular, it is well known that harmonic seeding schemes must contend with increasingly strict electron beam tolerances as the harmonic number increases. Initial errors that are insignificant compared to the seed wavelength may be large relative to a much shorter wavelength harmonic. For example, harmonic multiplication amplifies electron shot noise, which can overwhelm the external seeding source [6, 7, 8, 9]. More recently attention has turned to errors from the seed laser itself [5, 10, 11, 12, 13]. Without sufficient control of the initial seed laser phase, the x-ray pulse acquires longitudinal structure; if sufficiently far from the transform-limit, seeding may have little or no benefit compared to SASE FELs.

This paper focuses on the effects of laser phase errors on the seeded electron density, using both analytical methods [12] and simulations [5]. We also consider several potential

techniques for measuring and controlling laser phase in the UV spectrum.

SCHEMATIC DESCRIPTION OF HARMONIC PHASE MULTIPLICATION

As a simple example of seeding, we consider a High Gain Harmonic Generation (HG) scheme driven by a temporally flat-top laser pulse of wavelength, λ_L . The seeding scheme bunches the electrons both at the fundamental wavevector, $k_1 = 2\pi/\lambda_L$, as well as at higher harmonics $k_H = Hk_1$, for harmonic number H .

In a non-ideal laser pulse, the wavelength varies as a function of time; i.e. the pulse has non-flat phase. As the wavelength changes, the resulting separation of electron density spikes also shifts from the central wavelength, as illustrated in Fig. 1. Because the relative shift in frequency is the same at all harmonics, an increase in the fundamental frequency of Δk_1 will grow the harmonic bandwidth by $\Delta k_H \approx H\Delta k_1$.

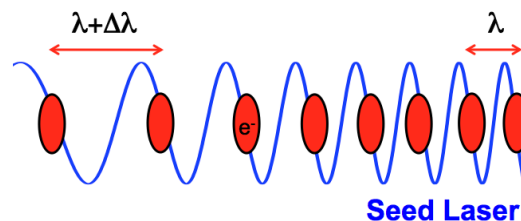


Figure 1: Cartoon illustrating the effect of seed phase errors on HG electron bunching. A time-varying wavelength in the seed laser (blue line) results in a varying separation of the bunched electrons (red bunches).

To quantify the effect of wavelength variation in the seed laser, we calculate the FEL's Time-Bandwidth Product (TBP), $TBP = c\Delta T_{FEL}\Delta k_{FEL}$, from the pulse duration, ΔT_{FEL} , bandwidth, Δk_{FEL} and speed of light, c . For a given spectral distribution, the minimal TBP corresponds to a transform-limited pulse. As the TBP grows, the seeded FEL characteristics revert to those of a SASE pulse. For a flat-top seed laser with a small linear variation in wavelength, all harmonics have the same pulse length, so we the TBP grows linearly with harmonic number.

HG WITH SPECTRAL PHASE ERRORS

Laser Phase Definition

Experimental laser measurements are predominantly spectral, so it is convenient to describe the laser pulse using

the electric field in the spectral domain

$$\tilde{\mathcal{E}}(k) = \tilde{E}(k)e^{-i\phi(k)}, \quad (1)$$

with spectral intensity, $\tilde{E}(k)$ and phase

$$\phi(k) = \sum_{n=2}^{\infty} \frac{\phi_n}{n!} (k - k_0)^n. \quad (2)$$

(We ignore the ϕ_0 and ϕ_1 terms, which represent the carrier-envelope offset and the envelope temporal delay respectively, and are not relevant to this analysis.) A transform-limited pulse by definition has minimal TBP and flat spectral phase, $\phi(k) = 0$. Non-ideal laser pulses will have non-negligible spectral phase, and these phase terms produce longer pulses with greater intensity fluctuation in the time domain; i.e. pulses farther from the transform limit.

Analytical approaches generally assume quadratic phase, and a laser pulse that is either much shorter [5, 12] or much longer [13] than the electron pulse. Due to the challenge of producing sufficient laser power at short wavelengths, in this paper we focus on the case of a short laser pulse.

Electron Phase Definition

To estimate the FEL radiation at wave vector k , we define the averaged electron bunching factor

$$b(k) \equiv \frac{1}{N_T} \sum_{j=1}^{N_T} e^{-ik\bar{z}_j}, \quad (3)$$

where the sum is over the final longitudinal position, \bar{z} , of all N_T electrons in the bunch. We can also define a local bunching factor by summing over a single wavelength slice of the beam. In this case, we change the normalization of Eq. 3 to the number of electrons in the local slice, $N_{\text{slice}}(z)$, giving

$$b_{\text{slice},k}(z) \equiv \frac{1}{N_{\text{slice}}(z)} \sum_{j=1}^{N_{\text{slice}}(z)} e^{ik\bar{z}_j}. \quad (4)$$

In HGHG and EEHG, the seeded bunching factor largely determines the FEL characteristics at saturation. For example, the length of the slice bunching, $b_{\text{slice},k}(z)$, determines the duration of the FEL pulse, ΔT_{FEL} . The width of a harmonic in the averaged bunching, $b(k)$, determines the FEL bandwidth, Δk_{FEL} . From the product of the RMS FEL duration, ΔT_{FEL} , and bandwidth, Δk_{FEL} , we find the TBP of the FEL.

We can also define a spectral phase of the electron bunch from the argument of the averaged bunching factor,

$$\phi_{e-}(k) = \text{Arg}[b(k)]. \quad (5)$$

The electron spectral phase is directly analogous to the laser spectral phase (Eq. 2).

Second Order Spectral Phase, Analytical Approach

For a pulse with Gaussian spectral amplitude of RMS width, σ_k , and second order spectral phase, ϕ_2 , the bunching factor can be found analytically. In the time domain this pulse has a Gaussian duration, σ_L , and second order temporal phase, α_2 , determined by the spectral equivalents, σ_k and ϕ_2 . Assuming a longitudinally uniform distribution with an energy spread of σ_p , the averaged bunching factor is [12]

$$b_H(\delta k) \propto \sigma_L e^{-H^2 r^2 (1+0.81H^{-2/3})^2 / 2A_0^2} \times G_H^{(\text{HG HG})}(\delta k \sigma_L / H, H\beta \sigma_L^2 / \lambda^2, r), \quad (6)$$

with

$$G_H^{(\text{HG HG})}(x, y, r) \equiv \int_{-\infty}^{\infty} d\xi e^{ix\xi + iy\xi^2} \times J_H \left[r(H + 0.81H^{-1/3})e^{-\xi^2/2} \right], \quad (7)$$

where $\beta \equiv \alpha_2 / 2k_L^2$ is the dimensionless second order phase and $r \sim 1$ optimizes the bunching factor near the peak of the laser pulse. From $b_H(\delta k)$ we can determine both the bandwidth, Δk_{FEL} and the spectral phase, $\phi_{e-}(k)$, as a function of harmonic number. Ref. [12] gives the full derivation of Eqs. 6 and 7.

Second Order Spectral Phase, Simulation

Numerical approaches can extend solutions to higher order spectral phase. Figures 2 and 3 show comparisons between analytical and numerical results. Figure 4 shows the spectral phase, $\phi_{e-}(k)$, for the first ten harmonics, calculated from both simulations and Eq. 6. When the seed pulse has quadratic phase, the electron bunching factor also shows quadratic phase. As expected, the phase increases as a function of harmonic number.

Pulse Shortening

The increase in TBP for Gaussian pulses is not as large as predicted for a flat-top pulse. The flat-top and Gaussian cases differ primarily due to the effect of harmonic pulse shortening, evident in Fig. 5. In a flat-top pulse, the FEL pulse length is independent of harmonic number. By contrast, Fig. 6 confirms that in HGHG from a Gaussian seed laser, the pulse length is approximately proportional to $H^{-1/3}$ [12]. Pulse shortening changes the harmonic spectral phase; while the fundamental bunching follows the seed laser amplitude and phase, the harmonic bunching samples phase only from the center of the seed pulse.

Arbitrary Spectral Phase, Simulation

Simulations allow study of realistic laser pulses that contain non-negligible spectral phase beyond the 2nd order. Figure 7 shows the 10th harmonic electron spectral phase,

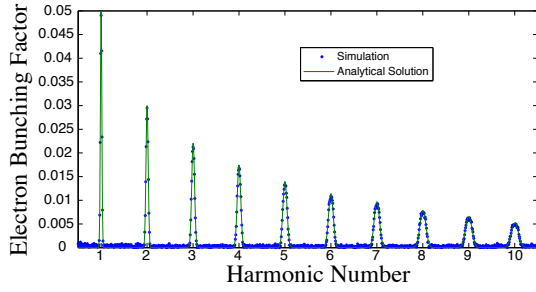


Figure 2: Electron bunching factor for a Gaussian seed laser pulse with quadratic phase. The seed laser pulse has phase $\phi(\sigma_k) = \pi$, amplitude $A_0 = 30\sigma_p$, and RMS bandwidth $\sigma_k/k_L = 10\%$. Amplitude of the bunching factor is small due to averaging over a long electron bunch of uniform length, $L = 10\sigma_L$ (Eq. 3). Simulated bandwidths (blue) reproduce the analytical result (Eq. 7 in green, scaled to match the bunching amplitude). As expected, the peaks broaden at higher harmonics.

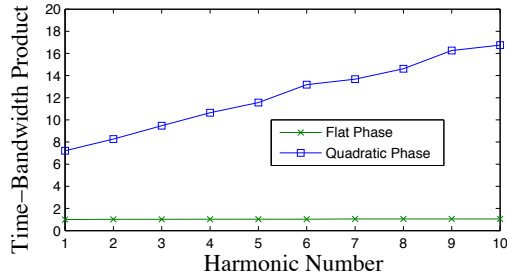


Figure 3: RMS TBP, $c\Delta T_{\text{FEL}}\Delta k_{\text{FEL}}$, for the electron bunching factor of Fig. 2. The TBP increases at higher harmonics (blue squares), but slower than would be expected from a flat-top pulse. For comparison, a transform-limited pulse with flat phase has minimal TBP at all harmonics (green stars).

$\phi_e(k)$, from seed lasers with 2nd through 5th order spectral phase. Note that odd order phases have less impact on the electron bunch than the even orders due to pulse shortening. Figure 8 illustrates the effect of pulse shortening for third order phase.

The loose constraints on odd order phase may aid in production of transform-limited pulses. For example, canceling only the even order seed laser phase will reduce the complexity of the optical setup. Alternatively, it may be beneficial to treat the laser phase as a total minimization problem; rather than separately minimizing each order, it is possible to collectively select all orders to minimize the TBP of the FEL. This collective approach is analogous to methods used in the production of transform-limited laser pulses [14, 15].

EEHG WITH SPECTRAL PHASE ERRORS

In EEHG, spectral phase on the seed laser affects the two modulation stages differently [16]. On the first laser pulse, spectral phase distorts the separation of the filaments, so

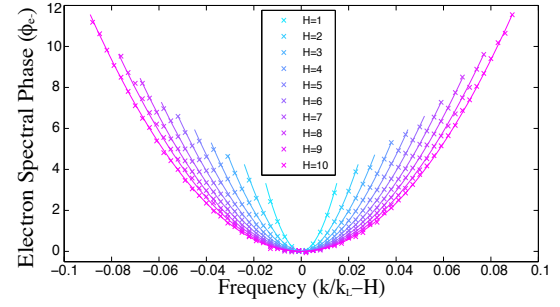


Figure 4: Spectral phase of the electron bunching factor from Fig. 2 for the first ten harmonics. Solid line calculated from Eq. 7, with crosses taken from simulations. At higher harmonics the curves are wider due to the increasing bandwidth.

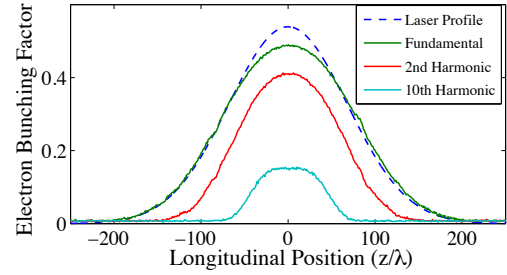


Figure 5: Slice electron bunching factor and laser E-field as a function of longitudinal position. Each bunching factor point corresponds to a slice of the electron bunch of width λ_L (Eq. 4).

that the density spikes do not fall exactly at the harmonic spacing (Fig. 9). The distortion reduces the bunching factor, but because the second laser still phase locks each set of density spikes, there is relatively little effect on the TBP.

The second stage of EEHG is similar to the HGHG process. Assuming a flat-top laser pulse in the first stage and a Gaussian pulse of length σ_{L2} in the second stage, the increase in electron bunching factor bandwidth is given by $G_H^{(\text{EEHG})}[\delta k\sigma_{L2}/H, (H+1)\beta\sigma_{L2}^2/\lambda^2]$ [12], with

$$G_H^{(\text{EEHG})}(x, y) \equiv \int_{-\infty}^{\infty} d\xi e^{ix\xi + iy\xi^2} \times J_{H+1}\left(r[(H+1) + 0.81(H+1)^{-1/3}]e^{-\xi^2/2}\right), \quad (8)$$

analogous to Eq. 7 for the case of HGHG. Figure 10 confirms the different effects of phase errors in the first and second laser stages.

PRACTICAL EXAMPLE

We conclude by simulating a practical example using an 800 nm laser pulse. Table 1 gives experimentally measured spectral parameters from an ultrafast Ti:Sapphire amplifier (the Coherent Legend Elite USX). The pulse length of 22 fs is close to the transform-limited (flat phase) pulse length of 20 fs. Despite the nearly transform-limited initial seed

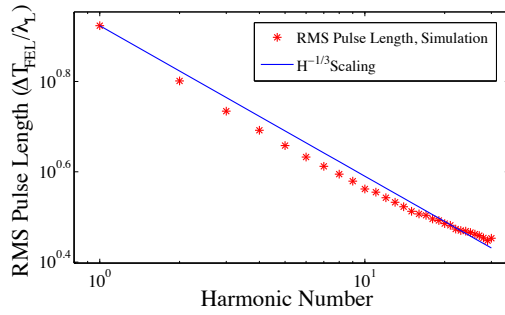


Figure 6: Pulse length as a function of harmonic number. Simulation pulse lengths determined from the electron bunching factor (stars) follow the expected $H^{-1/3}$ scaling (line).

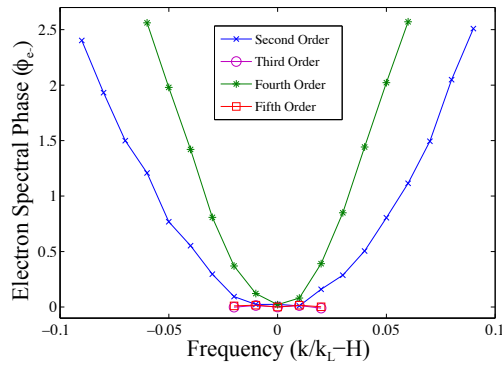


Figure 7: Electron spectral phase, ϕ_{e-} , at the 10th harmonic for seed laser pulses with 2nd through 5th order spectral phase. For each curve the spectral phase of the laser seed has $\phi(\sigma_k) = \phi_n \sigma_k^n / n! = 1$ (Eq. 2). The bandwidth, Δk_{FEL} , determines the plotted range; the odd order cases produce narrower bandwidths.

laser pulse, Fig. 11 shows that the electron bunching factor at the 30th harmonic is approximately three times the transform limit. From Fig. 12 we see that if the phase errors increase beyond the level of Table 1 by just a factor of two, the formerly transform-limited pulse starts to acquire temporal modulations.

Table 1: Measured parameters for a nearly transform-limited 800 nm pulse. The fourth order phase dominates the FEL performance.

Measured Laser Pulse	
Central Wavelength	800 nm
Bandwidth (FWHM)	73 nm
Pulse Duration	22 fs
Second Order Phase (GDD)	0.5 fs ²
Third Order Phase (TOD)	2.4×10^3 fs ³
Fourth Order Phase (FOD)	-4.6×10^4 fs ⁴
Fifth Order Phase (FOD)	-1.2×10^6 fs ⁵

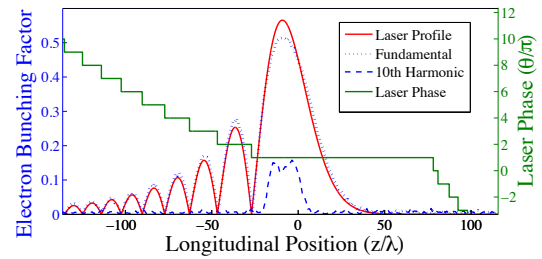


Figure 8: Slice bunching factor (Eq. 4) as a function of position for the fundamental and 10th harmonic. Third order spectral phase on the seed laser produces side pulses on the time-domain E-field (solid red line). The temporal phase (solid green line) is flat within each pulse, but jumps by π between pulses. The 10th harmonic bunching factor (dash blue line) exists only in the center of the largest pulse, and consequently does not pick up the third order phase.

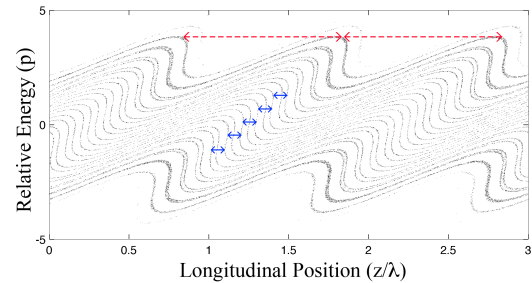


Figure 9: Schematic of EEHG phase space. Phase errors on the first stage distort the separation of density spikes within a single modulation wavelength (solid blue arrows), but the length of each group (dotted red arrows) is phase locked by the second stage. Phase errors on the second stage, by contrast, can change the final seeded wavelength.

MEASURING AND CONTROLLING UV LASER PHASE

At present there are numerous techniques for characterizing ultrafast laser pulses (see e.g. [17, 18]). Some of the most popular techniques are variations of Frequency Regime Optical Gating (FROG) [19] and Spectral Phase-Interferometry for Direct E-field Reconstruction (SPIDER) [20].

Both FROG and SPIDER were originally developed for the optical regime; the two methods rely on readily available nonlinear materials in the optical range to either gate (FROG) or interfere pulses (SPIDER) to reveal the spectral phase. However, in the last decade several groups have made progress in porting the techniques to shorter wavelengths. For example, the nonlinearity of the photoelectric effect can be used both FROG [21] and SPIDER [22]. It is also possible to apply the nonlinearity to the long wavelength drive pulse prior to generating the UV seed wavelength [23]. Both approaches have been used to demonstrate the feasibility of High Harmonic Generation (HHG) sources with flat spectral phase at wavelengths below 75 nm [21, 23].

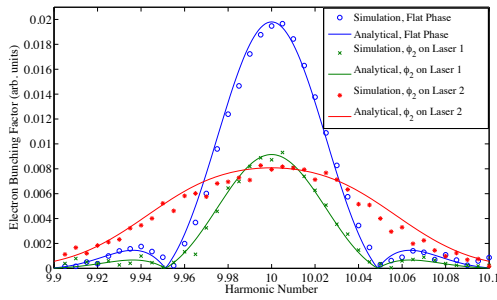


Figure 10: Averaged bunching factor for 10th harmonic EEHG with Gaussian envelope for both laser stages. Quadratic phase on the first seed laser ($\phi_2 \sigma_k^2 / 2 = 1$) reduces the bunching factor, but does not broaden the bandwidth. The same quadratic phase on the second seed laser increases the bandwidth and TBP as found for HHG. Solid lines show the numerical integral, Eq. 8.

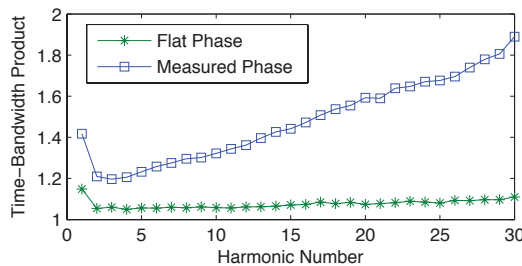


Figure 11: RMS TBP vs harmonic number for the pulse parameters given in Table 1. Even for this nearly transform-limited seed pulse, the TBP at the 30th harmonic (blue squares) is almost three times the transform-limited flat-phase case (green stars). Note that in [5] the stars were incorrectly labeled as 'quadratic' phase instead of 'measured' phase.

While recent results are promising, there is still a need for significant research and development of phase control techniques at the short wavelengths relevant to seeded x-ray FELs.

CONCLUSION

We have described the effect of seed laser phase on HHG and EEHG schemes. The electron bunching factor copies the seed laser spectral phase and the electron spectral phase increases with harmonic number, but pulse narrowing from the laser envelope decreases the phase growth, especially for odd order spectral phase. A realistic laser pulse in the optical regime will produce a seeded electron beam at the 30th harmonic with approximately three times the transform limit. We conclude that seeding near transform-limited pulses in the soft x-ray regime will require development of new methods for phase measurement and control of short wavelength lasers or HHG sources. The required level of phase control is on par with that currently available at 800 nm.

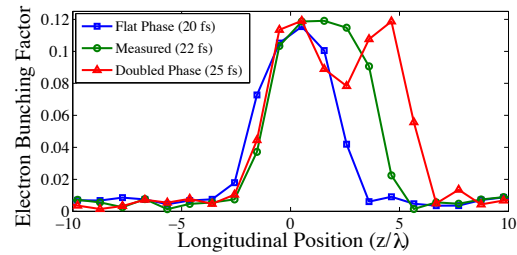


Figure 12: Slice electron bunching vs. time for parameters of Table 1. Bunching is shown for the 30th harmonic of laser pulses simulated with flat phase (blue squares), measured phase (green circles) and twice the measured phase (red triangles).

ACKNOWLEDGEMENTS

We thank Y. Feng, Z. Huang and P. Hering for helpful discussions. Work is supported by Department of Energy contract DE-AC02-76SF00515.

REFERENCES

- [1] P. Emma et al. *Nature Photonics*, 4:641–647, 2010.
- [2] H. Tanaka. In *Proceedings of IPAC2011*, San Sebastian, Spain, 2011.
- [3] H. Chapman et al. *Nature*, 470:73–77, 2011.
- [4] M. Seibert et al. *Nature*, 15:030702, 2012.
- [5] D. Ratner, A. Fry, G. Stupakov, and W. White *Phys. Rev. ST-AB*, 470:78–81, 2011.
- [6] E. L. Saldin, E. A. Schneidmiller, and M. V. Yurkov. *Optics Communications*, 202:169, 2002.
- [7] Z. Huang. In *Proceedings of the 2006 FEL Conference*, page 130, Berlin, Germany, 2006.
- [8] G. Stupakov. In *Proceedings of the 2010 FEL Conference*, Malmo, Sweden, 2010.
- [9] G. Stupakov, Z. Huang, and D. Ratner. In *Proceedings of the 2010 FEL Conference*, Malmo, Sweden, 2010.
- [10] G. Penn and M. Reinsch *Journal of Modern Optics* 58:16, 2011.
- [11] K. Hacker and H. Schlarb. Report TESLA-FEL 2011-05, DESY, 2011.
- [12] G. Stupakov. Report SLAC-PUB-14639, SLAC, 2011.
- [13] G. Geloni, V. Kocharyan, and E. Saldin. Report DESY 11-200, 2011.
- [14] S. Kane and J. Squier *J. Opt. Soc. Am. B*, 14:1237, 1997.
- [15] J. Squier, C.P.J. Barty, F. Salin, C. Le Blanc, and S. Kane. *Applied Optics*, 37:1638, 1998.
- [16] G. Stupakov. *Phys. Rev. Lett.*, 102:074801, 2009.
- [17] A. Monmayrant, S. Weber and B. Chatel *J. Phys. B.*, 43:103001, 2010.
- [18] I. A. Walmsley and C. Dorrer *Adv. Opt. Photon.*, 1:308-437, 2009.
- [19] R. Trebino, ed., *Frequency Resolved Optical Gating: the Measurement of Ultrashort Optical Pulses* Kluwer Academic, 2002.

- [20] C. Iaconis and I. A. Walmsley, *Opt. Lett.* 23, 792794, 1998.
- [21] A. Kosuge, T. Sekikawa, X. Zhou, T. Kanai, S. Adachi, and S. Watanabe. *Phys. Rev. Lett.*, 97:263901, 2006.
- [22] F. Quéré, J. Itatani, G. L. Yudin, and P. B. Corkum. *Phys. Rev. Lett.*, 90:073902, 2003.
- [23] Y. Mairesse, O. Gobert, P. Breger, H. Merdji, P. Meynadier, P. Monchicourt, M. Perdrix, P. Salières, and B. Carré. *Phys. Rev. Lett.*, 94:173903, 2005.